

# The structure of the energy bands and optical absorption in osmium

V. V. Nemoshkalenko, V. N. Antonov, V. I. Antonov, M. M. Kirillova, A. E. Krasovskii, and L. V. Nomerovannaya

*Institute of Metal Physics, Ural Scientific Center of the Academy of Sciences of the USSR, Sverdlovsk  
Institute of Metal Physics, Academy of Sciences of the Ukrainian SSR, Kiev*

(Submitted 18 June 1985)

Zh. Eksp. Teor. Fiz. **90**, 201–208 (January 1986)

The optical absorption of an osmium single crystal has been studied in the spectral range  $\hbar\omega = 0.08\text{--}40\text{ eV}$  ( $\lambda = 15\text{--}0.03\text{ }\mu\text{m}$ ). The energies of the main structural singularities of the interband optical conductivity  $\sigma$  were determined. The electron energy spectrum of osmium, the total and partial electron densities of state and also the frequency dependence of the interband conductivity  $\sigma(\omega)$  were calculated by the LMTO relativistic linear method in the constant transition matrix element approximation. Satisfactory agreement between the experimental and theoretical  $\sigma(\omega)$  curves was obtained. It was found that the formation of the main absorption bands for energies of 2–8 eV (1) and 10–25 eV (2) is due to the ( $d \leftrightarrow p$ ) and ( $d \leftrightarrow p, f$ ) type electron transitions, respectively.

Spectroscopic studies and theoretical calculations of the spectral properties, e.g., the dielectric permittivity  $\epsilon$ , are required in order to obtain reliable information on the electron band structure of metals. In recent years, such work has been carried out for many  $3d$ ,  $4d$ , and  $5d$  transition metals. Calculations of the frequency dependence of the dielectric permittivity  $\epsilon(\omega)$  ( $\omega$  is the angular frequency of the light wave) for the majority of metals with a cubic crystal lattice then showed satisfactory agreement with optical data and led to an understanding of the main laws governing the formation of the interband optical absorption spectra over a wide energy region.<sup>1–4</sup> Considerably less success was achieved in the interpretation of the optical properties of metals with a hexagonal lattice. Only individual theoretical calculations of  $\epsilon(\omega)$  have been carried out in this direction.<sup>5,6</sup>

The present work is devoted to an experimental and theoretical investigation of optical absorption in osmium. Osmium is a heavy transition metal with an unfilled  $5d$  shell, crystallizing with a hexagonal close-packed ( $hcp$ ) lattice. We reported earlier<sup>7</sup> on the existence of a very intense absorption band for photon energies  $\hbar\omega = 1.8\text{--}5\text{ eV}$ , produced by interband electron transitions. Cox *et al.*<sup>8</sup> found regions of increased reflection ( $R_{\text{max}} = 36\%$ ) in the  $\hbar\omega = 15\text{--}25\text{ eV}$  section of the spectrum in thin-film osmium specimens. We found even higher values of the reflectivity ( $R = 46\%$ ) in this energy range in a single-crystal specimen.<sup>9</sup> The existence of a region of heightened reflection in the spectral range indicated is evidence of an active interband excitation process at high photon energies and the presence of a high-energy absorption band. An interpretation of optical properties of osmium within the framework of a band calculation was not carried out earlier.

The aim of the present work was to study and theoretically analyze the interband absorption in osmium, and to investigate the laws governing the formation of the frequency dependence of the interband optical conductivity  $\sigma(\omega)$  and the establishment of the connection between its spectral features and the energy band structure.

## 1. EXPERIMENTAL RESULTS

### 1. Specimens and measuring technique

The osmium single-crystals had electrical resistivity ratios  $\rho_{273\text{ K}}/\rho_{4.2\text{ K}}$  equal to 540 and 1150. The specimens were obtained by electro-spark cutting of single-crystals along (1000) and (1100) faces. The accuracy of the orientation of the faces to within  $\pm 2^\circ$  was monitored by the Laue back-reflection x-ray method. The specimens were polished with a micropowder with  $5\text{ }\mu\text{m}$  size grains, and then electropolished to obtain a 14th class mirror finish in a 4–6% sodium hydroxide solution using a current density of  $2\text{ A/cm}^2$ . The cathode was of stainless steel. The absence of a strain-hardened layer on the surface after electropolishing was also checked by x-rays. Microtopograms taken from the surface of the (1000) and (1100) faces showed the presence of subgrains with an angular misorientation of  $30'$  and  $2^\circ$  respectively.

The optical constants, the refractive index  $n$  and the absorption coefficient  $k$ , were measured by the Beatty polarimetric method with an accuracy of 2–4%. As a uniaxial crystal in the optical ratio, hexagonal osmium has two components of the dielectric permittivity tensor:  $\epsilon_{\parallel} = (n_{\parallel} - ik_{\parallel})^2$  and  $\epsilon_{\perp} = (n_{\perp} - ik_{\perp})^2$ , corresponding to light waves propagating along ( $\mathbf{E} \parallel \mathbf{c}$ ) and perpendicularly ( $\mathbf{E} \perp \mathbf{c}$ ) to the crystal  $c$  axis. ( $\mathbf{E}$  is the electric vector of the plane-polarized light wave).

In the present work, the refractive indices  $n_{\perp}$ ,  $n_{\parallel}$  and the absorption coefficients  $k_{\perp}$ ,  $k_{\parallel}$  were determined in the wavelength range  $\lambda = 0.25\text{--}1.1\text{ }\mu\text{m}$  from measurements from the (1100) plane. The absolute values of  $n_{\perp}$ ,  $k_{\perp}$  and  $n_{\parallel}$ ,  $k_{\parallel}$  and their dispersion agreed with our earlier values obtained from the (1210) plane.<sup>7</sup> The values of  $n_{\parallel}$ ,  $k_{\parallel}$  in the infrared region  $\lambda = 1\text{--}8\text{ }\mu\text{m}$  were also determined from measurements from the (1100) plane. Numerical values of  $n_{\parallel}$  and  $k_{\parallel}$  are given in Table I. In addition, measurements were carried out of the optical constants of osmium in the spectral region  $\lambda = 0.25\text{--}15\text{ }\mu\text{m}$  from the basal (1000) plane. The latter, accurate to terms of order  $1/|\epsilon|$  compared with unity,

TABLE I. Optical constants of Os (1100) for the case E||c.

$\lambda, \mu\text{m}$	$n_{\parallel}$	$k_{\parallel}$	$\lambda, \mu\text{m}$	$n_{\parallel}$	$k_{\parallel}$	$\lambda, \mu\text{m}$	$n_{\parallel}$	$k_{\parallel}$
0.250	1.92	3.46	0.620	3.24	2.80	1.80	1.38	9.88
0.260	2.12	3.49	0.640	2.98	2.94	1.90	1.35	10.2
0.270	2.26	3.47	0.660	2.67	3.17	2.00	1.51	11.4
0.280	2.40	3.45	0.680	2.51	3.40	2.10	1.65	11.9
0.290	2.48	3.41	0.700	2.39	3.60	2.20	1.30	13.0
0.300	2.50	3.34	0.725	2.30	3.90	2.30	1.36	13.6
0.310	2.56	3.32	0.750	2.26	4.17	2.40	1.13	14.3
0.320	2.59	3.31	0.775	2.25	4.43	2.50	1.23	14.5
0.330	2.38	3.25	0.800	2.24	4.66	2.60	1.54	15.1
0.340	2.33	3.25	0.825	2.28	4.90	2.80	1.56	16.4
0.350	2.41	3.47	0.850	2.30	5.13	2.90	1.61	16.8
0.360	2.43	3.54	0.875	2.35	5.35	3.00	1.81	18.3
0.370	2.50	3.75	0.900	2.42	5.56	3.10	2.05	19.2
0.380	2.55	3.90	0.925	2.50	5.76	3.20	2.18	20.0
0.390	2.65	4.05	0.950	2.63	5.91	3.30	2.30	21.0
0.400	2.78	4.19	0.975	2.71	6.01	3.40	2.50	22.5
0.410	2.97	4.34	1.00	2.85	6.05	3.50	2.60	22.5
0.420	3.14	4.44	1.05	3.00	6.12	3.60	2.72	23.8
0.430	3.37	4.50	1.10	3.22	6.25	3.70	2.58	24.3
0.440	3.64	4.48	1.20	3.38	6.51	3.80	3.16	24.6
0.450	3.85	4.44	1.25	3.13	6.67	3.90	3.51	25.7
0.460	4.07	4.30	1.30	3.02	6.74	4.00	3.89	26.1
0.470	4.17	4.15	1.35	2.80	7.13	4.25	4.20	27.6
0.480	4.28	3.97	1.40	2.48	7.04	4.50	4.08	28.7
0.490	4.32	3.83	1.45	2.27	7.60	5.00	4.42	30.9
0.500	4.38	3.61	1.50	1.92	7.81	5.5	4.69	32.7
0.520	4.33	3.40	1.55	1.78	8.08	6.0	4.75	34.6
0.540	4.22	3.15	1.60	1.50	8.45	6.5	5.57	35.4
0.560	4.03	2.96	1.65	1.44	8.91	7.0	7.20	37.8
0.580	3.79	2.82	1.70	1.51	9.01	8.0	9.30	39.3
0.600	3.50	2.79	1.75	1.26	9.73	--	--	--

correspond to  $n_{\perp}$  and  $k_{\perp}$ . The dispersion dependences of the refractive index  $n_{\perp}(\omega)$  and absorption coefficient  $k_{\perp}(\omega)$ , obtained from measurements from the (1100) face (E1c) and the basal (1000) plane agreed completely, but in the latter case the values of  $n_{\perp}$  and  $k_{\perp}$  were somewhat higher,

evidently because of the higher quality of the electropolished (1000) plane. These numerical values are given in Table II.

The optical constants  $n_{\perp}$  and  $k_{\perp}$  of osmium in the energy range  $\hbar\omega = 5-40$  eV were evaluated by using the Kramers-Kronig relation from the results of the reflectivity

TABLE II. Optical constants of Os (1000).

$\lambda, \mu\text{m}$	$n_{\perp}$	$k_{\perp}$	$\lambda, \mu\text{m}$	$n_{\perp}$	$k_{\perp}$	$\lambda, \mu\text{m}$	$n_{\perp}$	$k_{\perp}$
0.240	1.53	3.29	0.850	2.81	2.15	3.10	2.31	14.2
0.248	1.63	3.55	0.900	2.42	2.53	3.20	2.38	14.4
0.253	1.67	3.64	0.950	2.12	3.00	3.30	2.50	14.6
0.265	1.97	3.98	1.00	1.94	3.32	3.40	2.38	15.1
0.280	2.13	3.93	1.05	1.62	3.77	3.50	2.57	15.5
0.288	2.49	3.98	1.10	1.47	4.37	3.60	2.87	15.7
0.296	2.76	4.15	1.15	1.37	4.82	3.70	2.68	15.8
0.302	2.87	3.85	1.20	1.22	5.17	3.80	2.35	16.4
0.312	3.04	3.73	1.25	1.20	5.45	3.90	2.60	16.4
0.334	2.89	3.81	1.30	1.00	5.83	4.00	2.78	17.3
0.370	2.94	3.97	1.35	1.00	6.18	4.25	3.17	18.2
0.380	3.02	4.09	1.40	0.85	6.51	4.50	3.19	19.7
0.390	3.12	4.19	1.45	0.75	6.68	4.75	3.24	20.1
0.400	3.28	4.35	1.50	0.91	6.84	5.00	3.98	23.4
0.410	3.44	4.50	1.55	0.84	7.19	5.25	4.30	24.6
0.420	3.66	4.56	1.60	0.76	7.60	5.50	4.47	25.1
0.430	3.98	4.74	1.65	0.95	7.77	5.75	4.78	25.9
0.440	4.27	4.71	1.70	0.85	8.07	6.00	5.20	27.8
0.450	4.57	4.68	1.75	0.80	8.27	6.50	5.42	29.0
0.475	4.99	4.33	1.80	0.89	8.42	7.00	6.70	32.6
0.500	5.43	4.01	1.85	0.80	8.81	7.5	7.60	33.7
0.525	5.70	3.58	1.90	0.76	9.18	8.0	7.93	35.8
0.550	5.86	2.99	2.00	0.65	10.3	8.5	8.40	36.7
0.575	5.60	2.53	2.10	0.88	10.8	9.0	9.10	37.5
0.600	5.48	2.16	2.20	0.93	11.3	10	10.2	39.0
0.625	5.17	1.94	2.30	1.10	11.7	11	9.59	39.8
0.650	4.83	1.87	2.40	0.90	12.0	12	10.1	42.0
0.675	4.49	1.79	2.50	1.29	12.7	13	12.5	49.9
0.700	4.23	1.67	2.60	1.30	13.0	14	16.6	57.5
0.750	3.79	1.64	2.90	1.60	13.2	15	17.5	61.7
0.800	3.37	1.71	3.00	1.97	13.8			

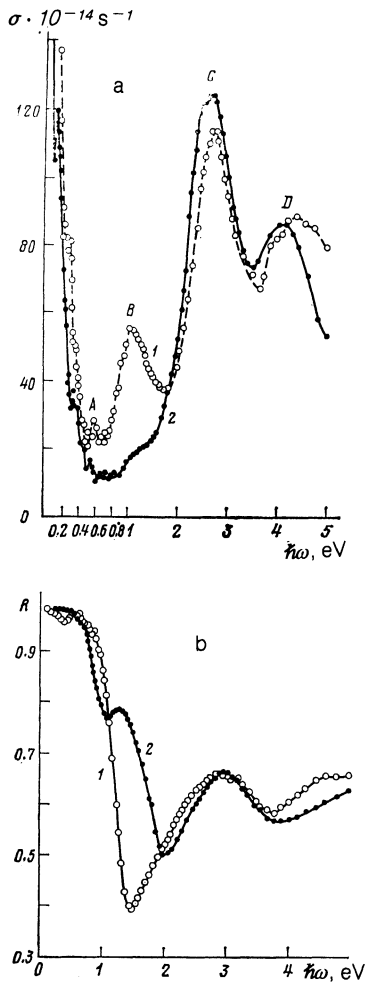


FIG. 1. The anisotropy of the optical conductivity  $\sigma$  (a) and of the reflective power  $R$  (b) of osmium: 1) ( $\mathbf{E} \parallel \mathbf{c}$ ), 2) ( $\mathbf{E} \perp \mathbf{c}$ ), specimen plane (1100). The values of  $\sigma_i$  and  $R_i$  in the spectral region  $\hbar\omega < 1.2$  eV are obtained by measurement from the (1000) plane.

obtained<sup>9</sup> on the same specimen, using synchrotron radiation. The calculation was carried out as described earlier.<sup>9</sup>

## 2. Optical conductivity

The optical conductivity of osmium,  $\sigma = nk\omega/2\pi$ , calculated from the values of the optical constants for two crystallographic directions  $\mathbf{E} \perp \mathbf{c}$  and  $\mathbf{E} \parallel \mathbf{c}$ , are shown in Fig. 1, a. In the energy range 2–5 eV, both curves,  $\sigma_{\perp}$  and  $\sigma_{\parallel}$ , have a very intense interband absorption band with two maxima, C and D. The increase in  $\sigma_{\perp}$  and  $\sigma_{\parallel}$  for  $\hbar\omega < 0.7$  eV is produced by the dominance of an intraband light absorption mechanism. However, there are interband contributions to the con-

ductivity in this spectral range. Thus, weak bumps are visible on the  $\sigma_{\perp}$  curve at energies 0.12, 0.38 and 0.54 eV and on the  $\sigma_{\parallel}$  curve at energies 0.22, 0.44 and 0.54 eV.

We found the greatest anisotropy of the optical conductivity at photon energies  $\hbar\omega = 0.5$ –1.8 eV. In this spectral region a very strong absorption peak B is formed on the  $\sigma_{\parallel}$  curve which is absent in the  $\sigma_{\perp}$  conductivity. A difference between the  $\sigma_{\perp}$  and  $\sigma_{\parallel}$  curves is also observed at energies greater than 2 eV, and is manifested in a different width and intensity of the two main absorption peaks, C and D.

Over the whole spectral range we studied,  $\hbar\omega < 5$  eV, anisotropy occurs in the reflectivity of osmium, which is largest at a wavelength  $\lambda = 0.823 \mu\text{m}$  ( $\hbar\omega = 1.5$  eV), where  $R_{\parallel} = 75\%$  while  $R_{\perp} = 40\%$  (Fig. 1, b).

## 2. CALCULATIONS

Calculations of the energy band structure, of the total  $N(E)$  and partial  $N_i(E)$  density of states, and also of the optical conductivity  $\sigma(E)$  were carried out by the relativistic linear LMTO method on the basis of the Dirac equation in the atomic sphere approximation.<sup>10</sup> The crystal potential was determined on the Mattheiss scheme<sup>11</sup> with total Slater exchange ( $\alpha = 1$ ). The parameters of the potential are given in Table III. In the expression for the crystal wave function and in the internal summing of the matrix element, terms up to  $\kappa = 3$  inclusively were used.

The electron energy spectrum of hexagonal osmium in the high symmetry directions of the Brillouin zone (BZ) are shown in Fig. 2. The structure and energy position of the dispersion curves  $E(k)$  agree well with Jepsen *et al.*,<sup>12</sup> in which a calculation by the LMTO method was carried out, based on a relativistic generalization of the Pauli equation. The difference is that according to Jepsen *et al.*,<sup>12</sup> there are hole pockets  $\Gamma 10h$  and  $L 7h$  at the points  $\Gamma$  and  $L$ . The present calculations, carried out as before<sup>13</sup> by the augmented plane wave method do not predict their existence. Hole pockets  $\Gamma 10h$  and  $L 7h$  are also not observed experimentally.<sup>14</sup>

Calculation of the partial densities of the  $s$ ,  $p$ ,  $d$  and  $f$  electron states shows that the  $d$  band is positioned in the energy interval  $E \simeq 0.35$ –1.15 Ry and has an intense maximum in the density of states above the Fermi level  $E_F$ , absent in the  $N_i(E)$  curves of the other type of symmetry. Two maxima can be distinguished on the  $N_p(E)$  curves. The first is positioned below  $E_F$  and is associated with  $s$ ,  $p$  and  $d$  hybridization. The second maximum, occupying the energy interval 1.5–2.5 Ry properly forms the  $p$  band. It is formed by the 13th to the 16th bands (see Fig. 2), which also have appreciable admixture of  $f$  states.

TABLE III. Crystal potential parameters for osmium.

Lattice type	Structural parameters a.u.		Atomic configuration	Radius of atmosphere a.u.
	$a$	$c$		
hcp	5.1692	8.1622	$5d_{3/2}^4 5d_{5/2}^2 6s_{1/2}^2$	2.4596

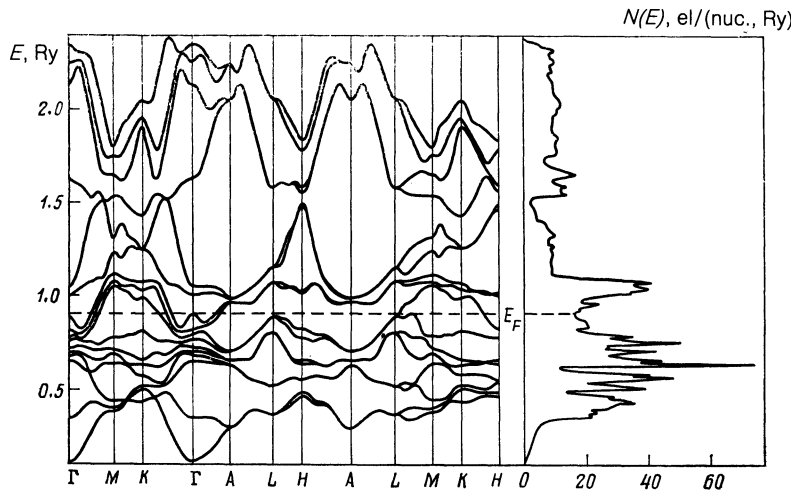


FIG. 2. The electron energy structure and the density of states  $N(E)$  of hexagonal osmium.

The interband optical conductivity  $\sigma(\omega)$  was calculated on the basis of the spectrum obtained in the constant transition-matrix element approximation according to the equation

$$\sigma(E) = \text{const } E^{-1} n_0(E). \quad (1)$$

Here  $n_0(E)$  is the optical density of states, which in the direct transition model is described by the expression (in a.u.)

$$n_0(E) = \frac{1}{\Omega_B} \sum_{ij} \int_{S_{ij}} \frac{dS}{|\nabla_{\mathbf{k}}[E_j(\mathbf{k}) - E_i(\mathbf{k})]|}, \quad (2)$$

where  $\Omega_B$  is the BZ volume, and  $S_{ij}$  is the surface limiting the region of reciprocal space  $V_{ij}$ , determined by the conditions

$$\begin{aligned} E_i(\mathbf{k}) &\leq E_F \leq E_j(\mathbf{k}), \\ E_j(\mathbf{k}) - E_i(\mathbf{k}) &\leq E. \end{aligned} \quad (3)$$

The calculation of  $\sigma(E)$  was carried out over the energy

range 0–30 eV. The partial interband contributions  $n_0^i(E)$  to the optical density of states was determined up to the 16th band.

The full  $N(E)$ , the partial  $N_i(E)$  and the optical  $n_0(E)$  density of states (the optical conductivity) were calculated using the tetrahedron method<sup>15</sup> over 95 points of 1/24 of the irreducible part of the BZ.

### 3. DISCUSSION OF THE RESULTS

We shall draw a comparison of the experimental and theoretical curves obtained for the optical conductivity of osmium.

The full curve of Fig. 3 shows the calculated results. The experimental results are shown by the dashed line. The ordinate axis scale for the theoretical  $\sigma(E)$  curve is chosen so that the height of the *C* and *D* maxima should agree on the theoretical and experimental curves.

It should first of all be noted that two regions of intense absorption are visible on the experimental  $\sigma(E)$  curve: 2–8

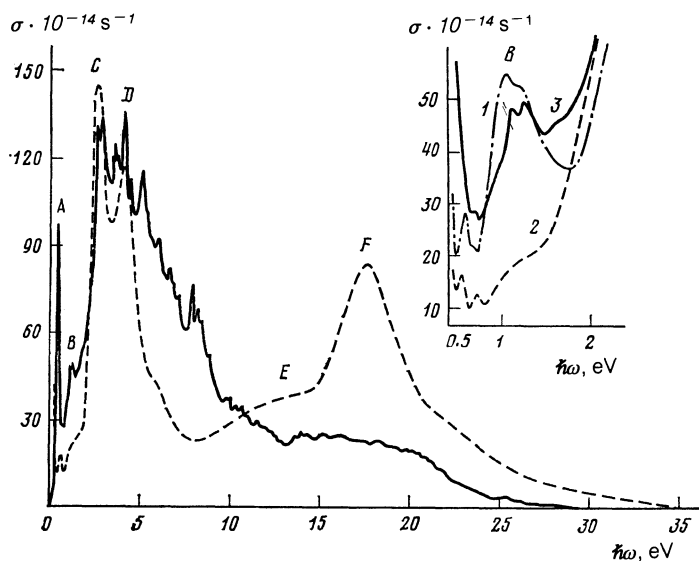


FIG. 3. The interband optical conductivity of osmium: full line—theory, dashed line—experiment from the (1000) plane. Inset: a section of the optical conductivity in the vicinity of peak *B*: 1)  $\sigma_{\parallel}^{\text{exp}}$ , 2)  $\sigma_{\perp}^{\text{exp}}$ , 3)  $\sigma^{\text{th}}$ .

eV (1) and 10–25 eV (2). Both absorption bands are associated with interband electron excitation, since the  $O_{III}$  ( $5p_{3/2}$ ) core level, which is 46 eV from the Fermi level in osmium, is not excited in the photon energy range considered.

The following facts have been established on the basis of the calculations and of the analysis of the partial contributions of the optical interband conductivity  $\sigma(E)$ .

1. The shape of the  $\sigma$  curve in the range of photon energies 2–8 eV (band 1) is determined by electron transitions between bands: 5→8,9, 6→7–11, 7→9→11 and 8→11,12. The largest contribution to the conductivity then comes from transitions involving the 5th, 6th and 7th bands which have planar cross sections in a number of BZ directions:  $\Gamma M$ ,  $MK$ ,  $\Gamma A$  and  $AH$  (Fig. 2). In particular, the  $C$  maximum is formed by the transitions 8→10,11 and 7→9,10. The double structure of the peak is noticeable on both the theoretical and experimental ( $E_1 = 2.58$  eV,  $E_2 = 2.75$  eV)  $\sigma$  curves. The  $D$  peak ( $E = 4.2$  eV) is formed by electron transitions between the bands 5→9,10, 6→10 and 7→10,11. Absorption band (1) on the whole is formed by ( $d \leftrightarrow p$ )-type electronic transitions.

2. The form of the  $\sigma$  curve in the photon energy range 10–25 eV (band 2) is determined by electronic transitions between bands 1–8→13–16, and the section  $E$  by transitions 1–7→11–14. We note that the partial contributions to the conductivity from transitions 1,2→13–16 are very insignificant, so that the spectral dependence of band 2 is mainly determined by ( $d \rightarrow p, f$ )-type transitions.

3. Theory predicts an absorption band  $B$  on the section  $\hbar\omega = 0.8$ –1.5 eV of the spectrum with a weak double structure at the vertex (inset to Fig. 3). It is formed by electronic transitions between bands 7→8 (the BZ direction  $ML$ ) and 8→9 (the  $\Gamma H$  direction). The partial contributions to the conductivity from these pairs of bands are maximal at energies 1–1.5 eV. A trace of the strong anisotropy in the interband transition probability of this band only appeared in the experiment for the direction  $E \parallel c$ . A “shoulder” was noted for the other crystallographic direction ( $E \perp c$ ) in this spectral range.

4. Weak low-energy absorption peaks on the  $\sigma_1$  curve at energies 0.12, 0.38 and 0.54 eV are formed by electronic transitions between bands 9→10 and 8→9 in the critical spectral regions [ $\nabla_k E_i(\mathbf{k}) = \nabla_k E_j(\mathbf{k})$ ], positioned along the  $\Gamma M$  and  $\Gamma K$  high-symmetry lines (Fig. 2). Transitions between the 7th and 8th bands also give a contribution to the low-energy absorption. The calculation predicts a threshold of optical absorption in osmium of  $\sim 0.1$  eV, which is associated with electronic transitions in the vicinity of the high-symmetry  $\Gamma A$  line between bands 9 and 10.

In accordance with experiment, two regions of heightened absorption were thus designated on the theoretical  $\sigma(E)$  curve: 2–8 eV (1) and 10–25 eV (2), due to electronic transitions of the ( $d \leftrightarrow p$ ) and ( $d \rightarrow p, f$ ) types respectively. The energy position of these bands, and also a number of their spectral features are, on the whole, in satisfactory agreement with the experimental results. However, the ratio of the intensities of these absorption bands on the theoretical

$\sigma(E)$  curve differs from that observed in experiment. The low-energy peak  $A$  is also raised on the theoretical curve. In addition, the calculation gives a whole array of peaks in the spectral range 5.5–9 eV, which are not found experimentally. These peaks are formed by electronic transitions from the filled part of the  $d$  band to empty states of the  $d$  or mixed ( $d-p$ ) symmetry, positioned 0.15 Ry above the Fermi level (2→9, 3,4→9,10, 1→7–10). The majority of these transitions are forbidden by selection rules in the dipole approximation. It can be suggested that taking account of the dependence of the transition matrix element on the wave-vector  $\mathbf{k}$  would appreciably improve the agreement between the experimental and theoretical  $\sigma(\omega)$  curves; in particular it would reduce the intensity of the peaks on the 5.5–9 eV section of the spectrum and change the ratio of the intensities of the absorption bands (1) and (2) on the theoretical curve. In addition, the energy band model of hexagonal osmium itself also requires further refinement and development.

In conclusion, we note that among transition  $d$  metals, osmium has an anomalously high interband conductivity. For example, in comparison with ruthenium,<sup>16</sup> which is its isostructural and isoelectronic analog, the absorption intensity in osmium at the maximum of band (1) is one and a half times higher. This is connected with the particular structure of the energy spectrum of Os, namely with the existence of an almost parallel behavior of the energy bands [the cases of  $\nabla_k E_j(\mathbf{k}) = \nabla_k E_i(\mathbf{k}) = 0$  and  $\nabla_k E_j(\mathbf{k}) = \nabla_k E_i(\mathbf{k})$ ] in several BZ directions:  $\Gamma M$ ,  $MK$ ,  $\Gamma A$ ,  $LH$  and  $HA$  (Fig. 2).

The authors are grateful to V. A. Elenskii for providing the osmium single-crystal and to V. A. Sazonova for the x-ray diffraction analysis.

<sup>1</sup>C. S. Wang and J. Callaway, Phys. Rev. B **9**, 4897 (1974).

<sup>2</sup>N. E. Christensen and B. Feuerbacher, Phys. Rev. B **10**, 2349 (1974).

<sup>3</sup>J. Yamashita, Y. Kubo, and S. Wakoh, J. Phys. Soc. Jpn. **42**, 1906 (1977).

<sup>4</sup>M. M. Kirillova, L. V. Nomerovannaya, V. G. Topol'skii, and V. P. Shirokovskii, Fiz. Met. Metalloved. **52**, 530 (1981) [Phys. Met. and Metallogr. (GB) No. 3, 66 (1981)].

<sup>5</sup>N. I. Kulikov and E. T. Kulatov, J. Phys. F **12**, 2267 (1982).

<sup>6</sup>N. I. Kulikov and M. V. Magnitskaya, Fiz. Nizk. Temp. **10**, 832 (1984) [Sov. J. Low Temp. Phys. **10**, 435 (1984)].

<sup>7</sup>M. M. Kirillova, L. V. Nomerovannaya, G. P. Kovtun, and V. A. Elenskii, Opt. Spektrosk. **52**, 682 (1982) [Opt. Spectrosc. (USSR) **52**, 407 (1982)].

<sup>8</sup>J. T. Cox, G. Hass, J. B. Ramsey, and W. R. Hunter, J. Opt. Soc. Am. **63**, 435 (1973).

<sup>9</sup>E. S. Gluskin, A. V. Druzhinin, M. M. Kirillova, V. I. Kochubei, L. V. Nomerovannaya, and V. M. Maevskii, Opt. Spektrosk. **55**, 891 (1983) [Opt. Spectrosc. (USSR) **55**, 537 (1983)].

<sup>10</sup>V. V. Nemoshkalenko, A. E. Krasovskii, V. N. Antonov, V. N. Antonov, U. Fleck, H. Wonn, and P. Ziesche, Phys. Status Solidi B **120**, 283 (1983).

<sup>11</sup>L. F. Mattheiss, Phys. Rev. A **133**, 1399 (1964).

<sup>12</sup>O. Jepsen, O. K. Andersen, and A. R. Mackintosh, Phys. Rev. B **12**, 3084 (1975).

<sup>13</sup>V. V. Nemoshkalenko, V. N. Antonov, and V. N. Antonov, Fiz. Nizk. Temp. **7**, 992 (1981) [Sov. J. Low Temp. **7**, 481 (1981)].

<sup>14</sup>G. N. Kamm and J. R. Anderson, Phys. Rev. B **2**, 2944 (1970).

<sup>15</sup>G. Lehmann and M. Taut, Phys. Status Solidi B **54**, 469 (1972).

<sup>16</sup>M. M. Kirillova, L. V. Nomerovannaya, M. M. Noskov, N. B. Gorina, V. P. Polyakova, and S. M. Savitskii, Fiz. Tverd. Tela (Leningrad) **20**, 1718 (1978) [Sov. Phys. Solid State. **20**, 994 (1978)].

Translated by R. Berman